Performance of small pore microchannel plates

O. H. W. Siegmund, M.A. Gummin,
T. Ravinett, S.R. Jelinsky, and M. Edgar

Space Sciences Laboratory, University of California, Berkeley, CA 94720

1.0 ABSTRACT

Small pore size microchannel plates (MCP's) are needed to satisfy the requirements for future high resolution small and large format detectors for astronomy. MCP's with pore sizes in the range 5μm to 8μm are now being manufactured, but they are of limited availability and are of small size. We have obtained sets of Galileo 8μm and 6.5μm MCP's, and Philips 6μm and 7μm pore MCP's, and compared them to our larger pore MCP Z stacks. We have tested back to back MCP stacks of four of these MCP's and achieved gains $>2x10^7$ with pulse height distributions of <40% FWHM, and background rates of <0.3 events sec^{-1} cm^{-2}. Local counting rates up to ≈100 events/pore/sec have been attained with little drop of the MCP gain. The bare MCP quantum efficiencies are somewhat lower than those expected, however. Flat field images are characterized by an absence of MCP fixed pattern noise.

Keywords: microchannel plate, UV, spectroscopy

2.0 SMALL PORE MICROCHANNEL PLATES

High spatial resolution (<15μm) is essential for future high resolution imaging and spectroscopy applications (FUSE)[1]. Currently, the size of the MCP pores is a significant limiting issue. Our current delay line readouts have resolutions of <15μm FWHM and <1μm electronic binning (Fig 1), and we can observe[2] the pore position "quantization" effects for MCP's with the standard pore sizes of 10μm (12μm center-center) or 12.5μm (15μm center-center).

A number of small pore (6μm to 8μm) MCP's were obtained from two manufacturers, and these are described in Table I. In each case, except for the 8μm MCP's, the MCP's were used in a back to back stack of 4 MCP's. This was done to ensure high saturated gain and tight pulse height distribution necessary for high resolution imaging detector systems. The 8μm MCP's were used in a Z stack configuration.

Table I. Small pore MCP specifications

Pore size	MCP size	L:D ratio	Resistance	Bias angle	Manufacturer
6μm	25mm	55:1	≈35MΩ	6°	Philips
6.5μm	33mm	50:1	≈60MΩ	12°	Galileo
7μm	25mm	50:1	≈100MΩ	6°	Philips
8μm	25mm	80:1	≈90MΩ	12°	Galileo

The MCP's were mounted in a brazed metal-ceramic detector body with a circumferential spring clamping arrangement for the MCP stack. The detector scheme is functionally similar to other devices that we have implemented in various space programs. The incoming UV photons are detected by the MCP channel walls, ejecting photoelectrons which impact the walls of MCP pores causing a charge avalanche with an overall charge multiplication of $\approx>10^7$. The field of view (18mm for the 25mm MCP's, and 25mm for the 33mm MCP's) is defined by an output aperture mask placed under the MCP stack. The brazed detector body is attached to a vacuum flange, that also has electrical feedthroughs to which the wedge and strip readout anode is mounted with a ≈10mm MCP to anode gap.

0-8194-2196-0/96/$6.00

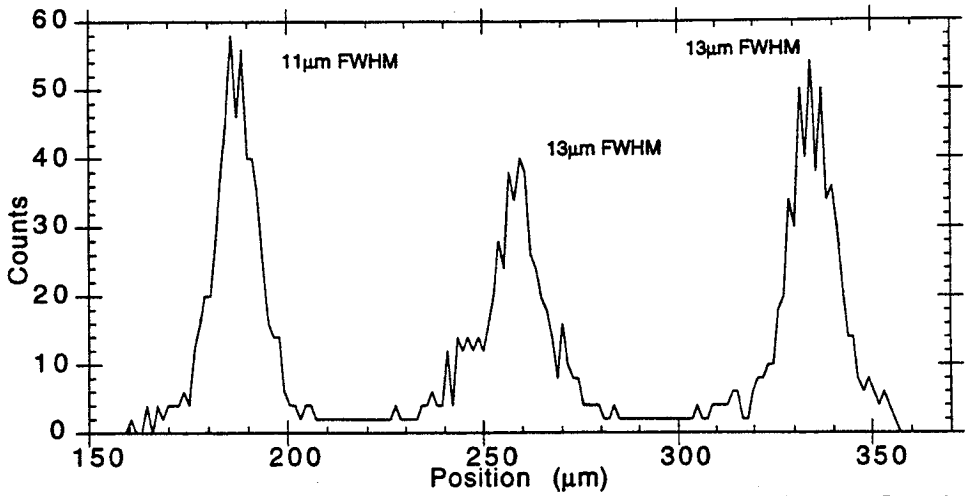

Figure 1. Histograms of three 10μm pinhole images taken with a 95mm x 15mm helical double delay line anode using a Z stack of 10μm pore (12μm centers) MCP's

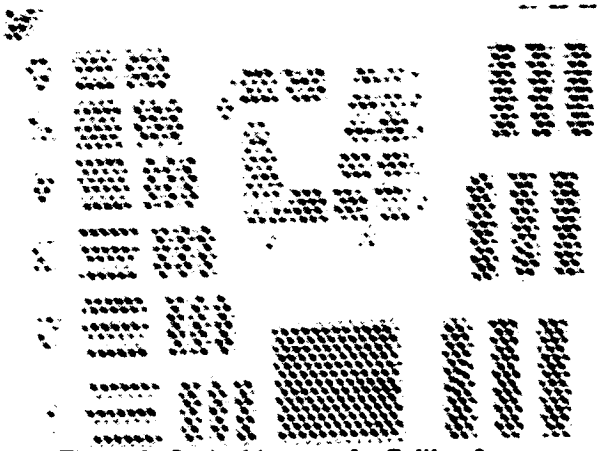

Figure 2. Optical image of a Galileo 8μm pore MCP with a 1952 air force test mask in contact

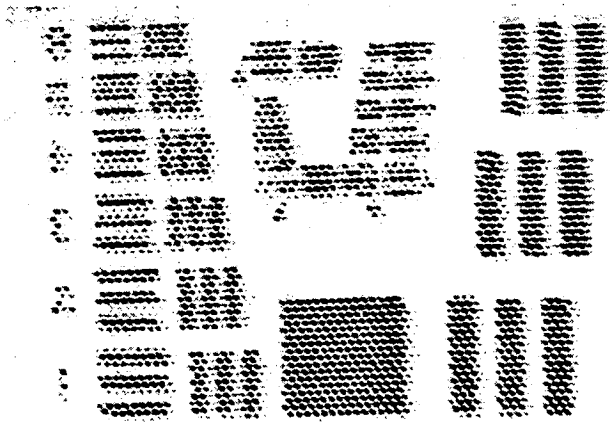

Figure 3. Optical image of a Philips 7μm pore MCP with a 1952 air force test mask in contact

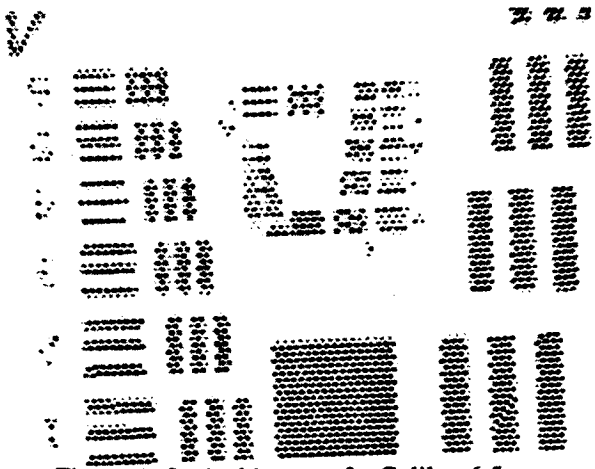

Figure 4. Optical image of a Galileo 6.5μm pore MCP with a 1952 air force test mask in contact

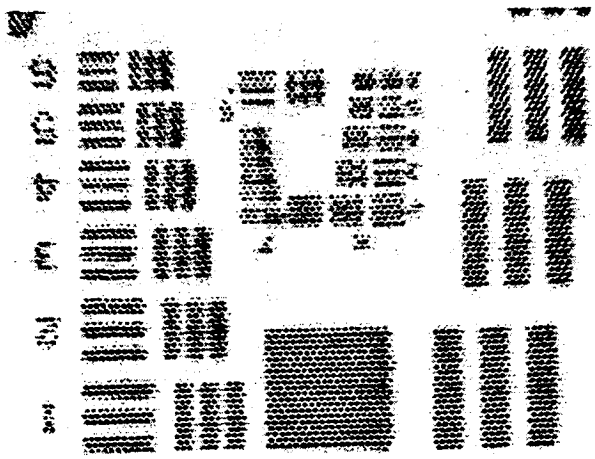

Figure 5. Optical image of a Philips 6μm pore MCP with a 1952 air force test mask in contact

To evaluate the limiting resolution of small pores we have also microscopically examined the small pore MCP's with a visible light back illumination through an Air Force resolution test mask (Figs. 2 to 5). As the size of the MCP pores reduces, the finer a resolution pattern can be resolved. 8μm MCP's can just resolve the 28 lp/mm pattern, but the 6μm MCP's can resolve the 40 lp/mm pattern. Small pore MCP's will hopefully eventually support a wide range of future instruments, providing better resolution performance and reducing the effects of MCP fixed pattern noise for critical applications such as high resolution spectroscopy.

3.0 MICROCHANNEL PLATE PERFORMANCE

3.1 Microchannel plate gain, pulse height distribution

The small pore 4 MCP stacks were generally tested under conditions where the entire field of view was uniformly illuminated with 2537Å light (Hg vapor lamp). The results of these tests show variations in performance from stackup to stackup, and often these differences have been due to gaps between the MCP's caused by individual MCP warpage. We have in some cases restacked the MCP's a number of times to ensure that there are no gain variations across the field of view. The pulse height spectra are gaussian in shape, demonstrating gain saturation. The gain and pulse height results for the Philips 7μm MCP's are shown in Figures 6 and 7. Gain of $>2 \times 10^7$ is achievable, which is not surprising given a four MCP stack. The pulse height distributions (PHD's) were quite good (≈40% FWHM), as indicated by the narrow distributions in Figures 6 and 7. The 4 MCP stacks of low L/D MCP's have fairly tight PHD's even at low gains, compared with more commonly used Z stacks of 80:1 L/D MCP's. This is an advantage for the discrimination of background events and reduction of the dynamic range necessary for imaging electronics. Using a beam of 256Å radiation covering about 15% of the field of view, PHD's of ≈33% FWHM were obtained.

The Galileo 6.5μm 4 MCP stack was more difficult to stack to obtain a tight PHD. The gain is not fully saturated at 2×10^7, and gains in excess of 3×10^7 were reached (Fig. 8) with pulse height distributions of ≈85% FWHM (Fig. 9). There was always a slightly higher gain in the center of the field of view, indicating slight MCP warpage. With all the small pore MCP stacks this is a potential problem since the solid edges are slightly thicker than the active pore area. The Philips 6μm pore MCP stack did not perform quite as well as the 7μm MCP's. The gains reached were again very high ($>3 \times 10^7$) (Fig. 10), and the PHD's were always between 55% and 50% FWHM (Fig. 11).

3.2 Background rate

The background rate and spatial distribution was assessed for each MCP type. Since the MCP field of view was open to the vacuum tank for all these tests there is a slight contribution due to stray ions in the tank. This is visible as a small "bump" in the background PHD on the background vs threshold plots. The spatial distribution for a 2200 sec integration of background events for the 7μm pore Philips MCP stack is shown in Figure 12. As expected from ^{40}K β decay in the glass, the distribution is essentially uniform. We observe a negative exponential pulse height distribution for background events with <0.35 events cm^{-2} sec^{-1} for a threshold of ≈10% of the modal gain (Fig. 13). The overall background rate is ≈0.23 events cm^{-2} sec^{-1} when the PHD peak due to tank ions is subtracted. This is lower then the rate (≈0.5 events cm^{-2} sec^{-1}) for intrinsic β decay MCP noise[3,4] for ^{40}K in the Philips glass in Z stack 80:1 MCP configurations. Since the 7μm MCP's are much thinner, there is less glass and hence less β decay MCP noise contributing to the intrinsic background rate. The 4 MCP 6μm Philips stack has a similar background rate behavior (Fig. 14). Again, if the tank noise peak is removed we get a rate of ≈0.27 events cm^{-2} sec^{-1} which is similar to the 7μm MCP performance. Thus one advantage of smaller pore MCP's is a reduced background rate at the same gain level, when compared to larger pore MCP's. The Galileo 6.5μm MCP's had a background rate of ≈0.53 events cm^{-2} sec^{-1} for a threshold of ≈25% the modal gain (Fig. 15). The Galileo MCP's had a higher incidence of low amplitude hot spots for these

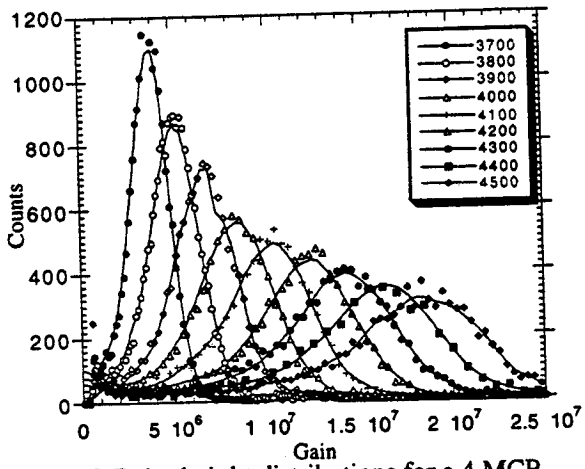

Figure 6. Pulse height distributions for a 4 MCP stack of Philips 7μm pore 50:1 L/D MCP's.

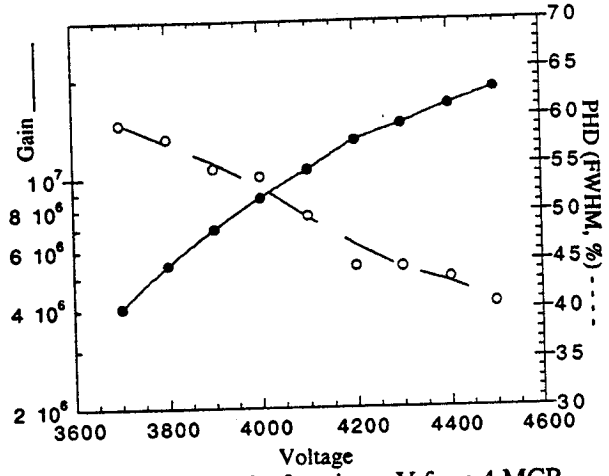

Figure 7. Pulse height & gain vs V for a 4 MCP stack of Philips 7μm pore 50:1 L/D MCP's.

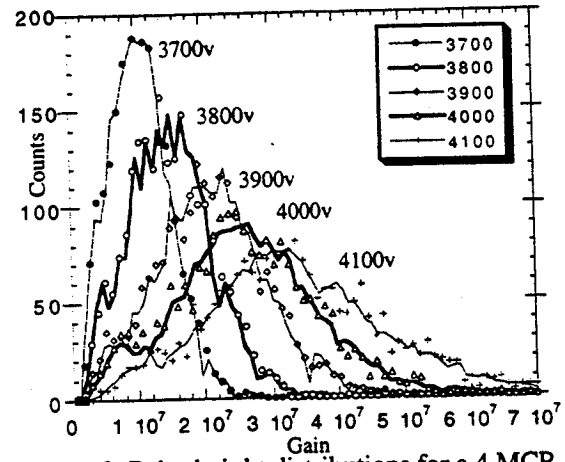

Figure 8. Pulse height distributions for a 4 MCP stack of Galileo 6.5μm pore 50:1 L/D MCP's.

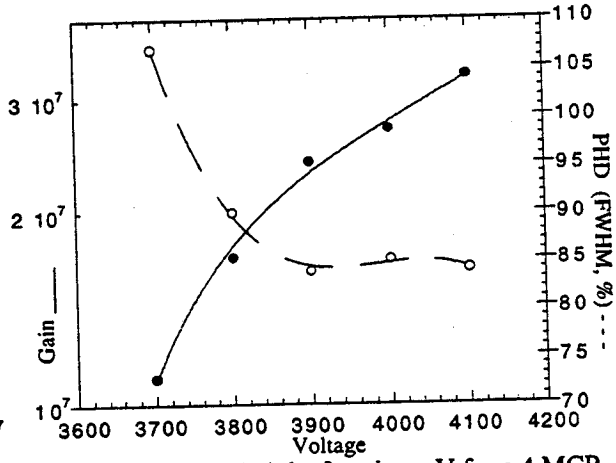

Figure 9. Pulse height & gain vs V for a 4 MCP stack of Galileo 6.5μm pore 50:1 L/D MCP's.

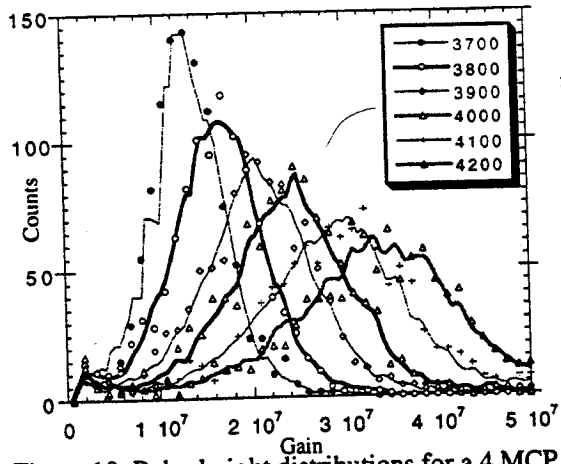

Figure 10. Pulse height distributions for a 4 MCP stack of Philips 6μm pore 55:1 L/D MCP's.

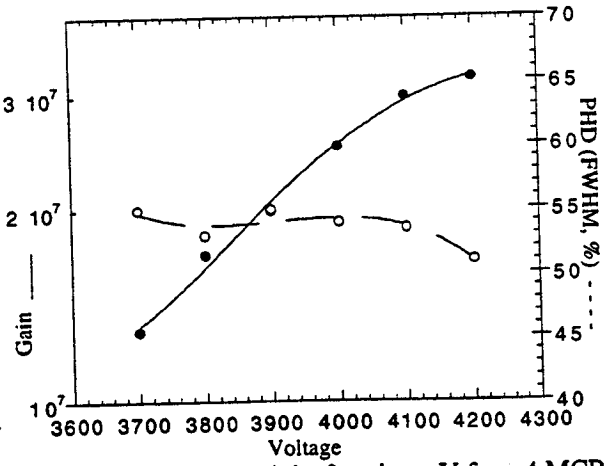

Figure 11. Pulse height & gain vs V for a 4 MCP stack of Philips 6μm pore 55:1 L/D MCP's.

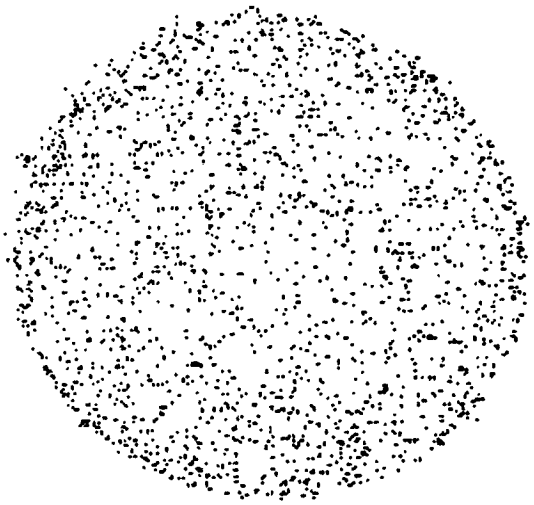

Figure 12. Background event image for a 4 MCP stack of Philips 7μm pore 50:1 L/D MCP's.

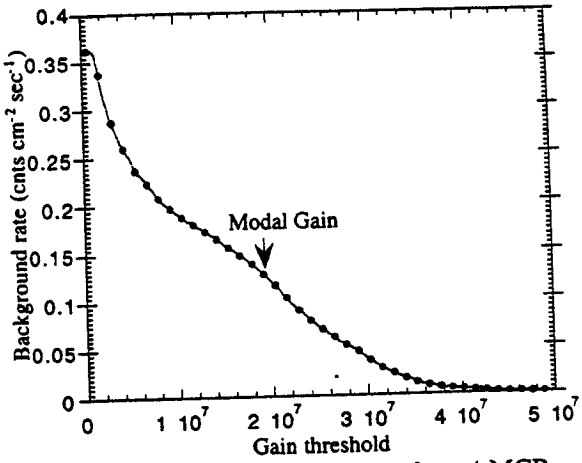

Figure 13. Background event rate for a 4 MCP stack of Philips 7μm pore 50:1 L/D MCP's.

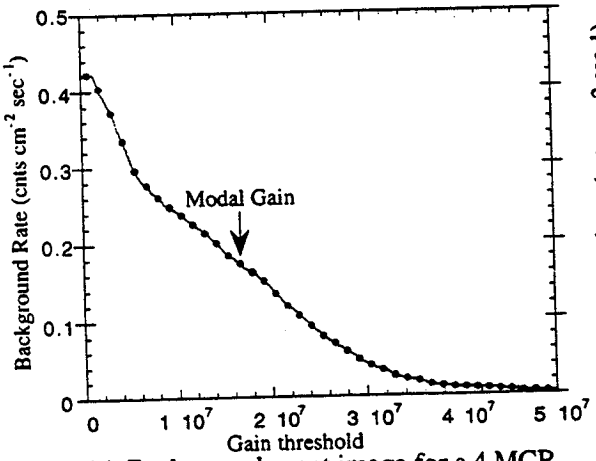

Figure 14. Background event image for a 4 MCP stack of Philips 6μm pore 50:1 L/D MCP's.

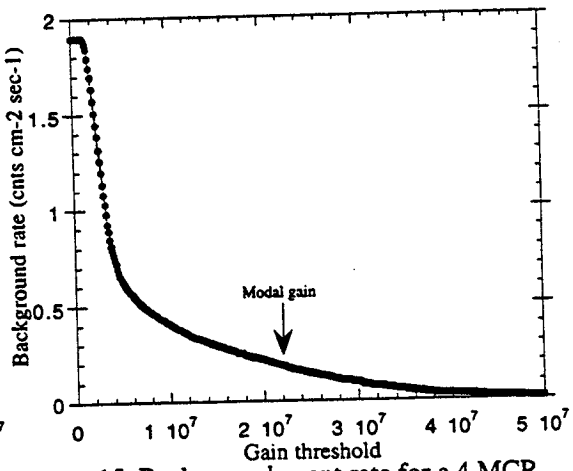

Figure 15. Background event rate for a 4 MCP stack of Galileo 6.5μm pore 55:1 L/D MCP's.

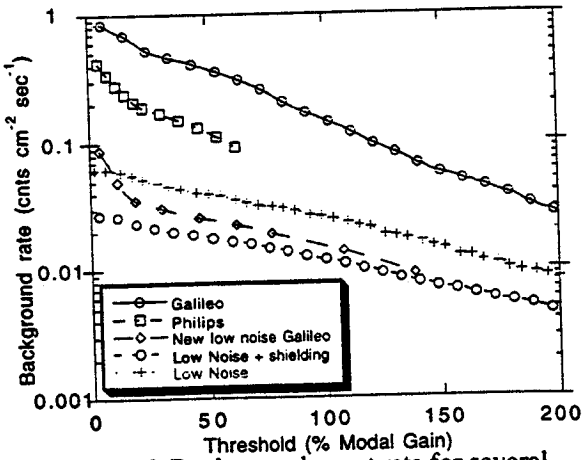

Figure 16. Background event rate for several stacks of MCP's as described in the text.

particular MCP's, which increased the rate at small thresholds. The overall rate of ≈0.53 events cm^{-2} sec^{-1} is about a factor of two higher than the standard Philips glass because ^{87}Rb is present rather than ^{40}K. The background rates for standard Philips (12μm) and Galileo (10μm) 80:1 Z stacks is shown in Fig.16. These are compared with an early batch of low noise Galileo 10μm MCP's with and without lead shielding. A recent result with new Galileo low noise glass is also included. These are 95 x 20mm curved surface MCP's in a Z stack of 3 x 80:1 MCP's for the FUSE explorer satellite. This result is very encouraging, with rates of <0.04 events cm^{-2} sec^{-1} at ≈20% modal gain threshold (without lead shielding). If small pore MCP's can be made from this material we expect very low intrinsic background rates (<0.02 events cm^{-2} sec^{-1}).

3.3 Counting rate performance

At high local event rates there is a progressive drop in the MCP stack gain and a degradation of the pulse amplitude distribution[5,6,7] due to the finite response time of MCP channel(s). The counting rate limit is proportional to the resistance of the MCP's, and is also dependent on the area illuminated. Only the Philips 6μm MCP's were low in resistance, so these were chosen for rate dependence tests. The 6μm MCP's have resistance in the range 170MΩ/cm^2 (≈35MΩ per MCP), which is slightly less than the MCP's used for the SOHO satellite[8]. Tests were made to evaluate the response to high local counting rate conditions such as those in some astronomical spectroscopy and imaging experiments. The high local counting rates on the MCP were generated using a variable flux from a pen ray lamp to illuminate a pinhole mask with 10μm 25μm, 50μm and 75μm pinholes. The gain as a function of local counting rate for the Philips 6μm 4 MCP stack is shown in Figure 17. The results show that the MCP gain remains stable up to ≈100 events $pixel^{-1}$ $sec^{-1}$for the 10μm and 25μm pinholes. So for this size input function the high local rates cause no loss of events or resolution degradation. For the 50μm holes the gain drop is ≈30% at ≈100 events $pore^{-1}$ sec^{-1}, and the gain drop is ≈70% at ≈100 events $pore^{-1}$ $sec^{-1}$for the 75μm pinholes. The PHD behavior (Fig. 18) for the 10μm and 25μm pinholes is essentially independent of the counting rate, with only a hint of broadening at ≈100 events $pore^{-1}$ sec^{-1}. Both the 50μm holes and the 75μm pinholes show significant PHD broadening at the higher counting rates. The 75μm pinhole PHD's begin to broaden at even a few counts $pore^{-1}$ sec^{-1}. These effects are essentially in accord with earlier observations of the dependence on the illuminated area[7]. One must also appreciate that a large number of pores are affected at the output MCP of the stack, and it is here where the charge extraction is largest and limitation occurs. It is also important to note that, for example, the counting rate in the 25μm pinhole at 100 events $pore^{-1}$ sec^{-1} is over 1000 events sec^{-1}, which is a significantly high rate.

3.4 Quantum detection efficiency

The quantum detection efficiency (QDE) of the bare 6μm, 6.5μm, 7μm and 8μm MCP's were measured as part of the overall characterization. The QDE vs wavelength properties were measured in an ultra high vacuum chamber at ≈10^{-6} torr with the MCP detector mounted such that the incident angle was ≈13° to the MCP pore axis. Monochromatic radiation was provided by a gas discharge hollow cathode source in combination with a 1m grazing incidence monochromator. After corrections are made for the contribution of the background radiation the absolute QDE's are derived from flux measurement comparisons with a reference standard. The choice of reference standard depends on wavelength measured; a NIST ultraviolet windowless photodiode, or a NIST far ultraviolet windowed photodiode were employed. The accuracy of the absolute QDE measured is determined largely by the accuracy of the reference standards. The NIST EUV photodiode has a most probable error of 10% from 68Å to 1216Å and the NIST far ultraviolet photodiode has a most probable error of 10% from 1216Å to 2537Å.

The results presented in Figure 19 show that the efficiencies for the Philips MCP's are slightly lower than expected compared to other bare MCP data[9] which we consider more "normal". The same kind of problem was also apparent (Fig. 20), although less severe, for the Galileo MCP's. The open area ratio of

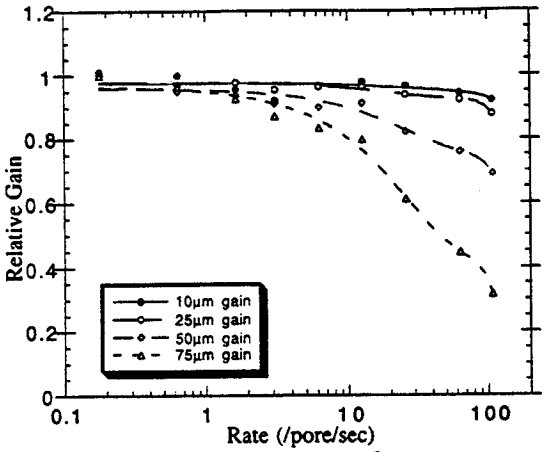

Figure 17. Gain vs counting rate & spot area for a 4 MCP stack of Philips 6µm pore MCP's

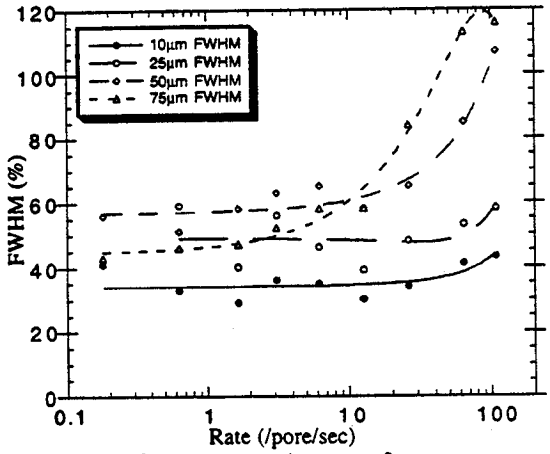

Figure 18. Gain vs counting rate & spot area for a 4 MCP stack of Philips 6µm pore MCP's

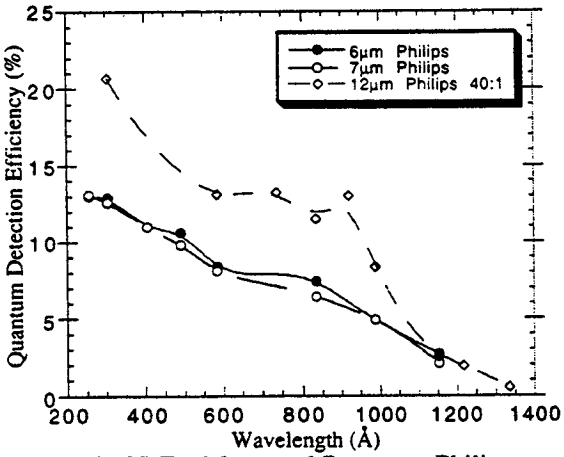

Figure 19. QDE of 6µm and 7µm pore Philips MCP's as a function of wavelength.

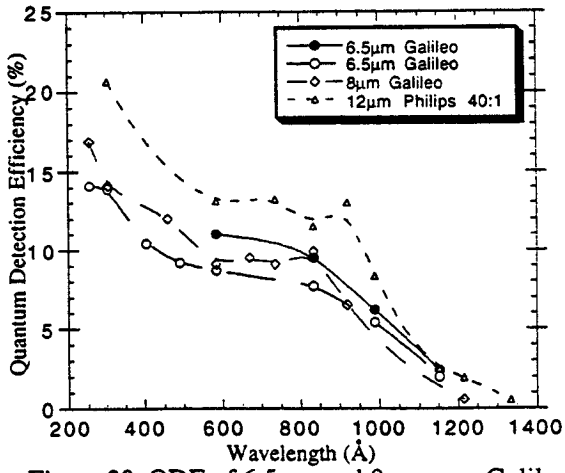

Figure 20. QDE of 6.5µm and 8µm pore Galileo MCP's as a function of wavelength.

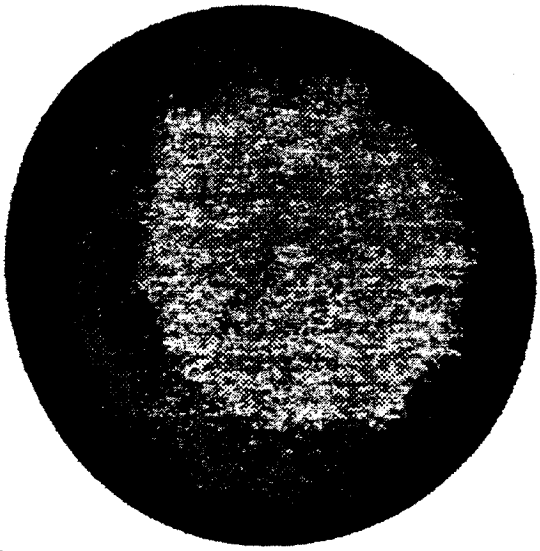

Figure 21. Flat field image for a 4 MCP stack of Philips 6μm pore MCP's.

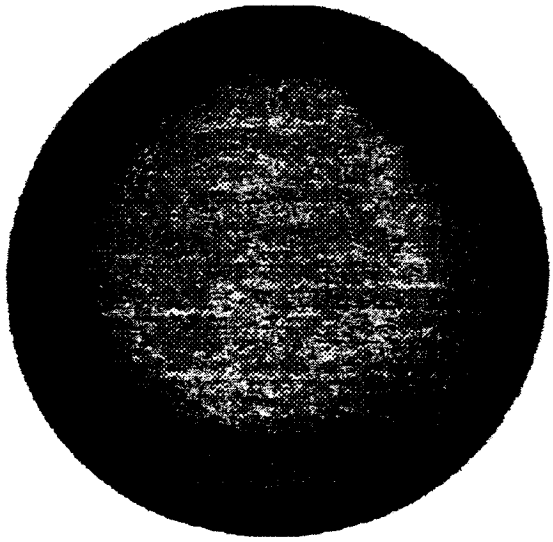

Figure 22. Flat field image for a 4 MCP stack of Philips 7μm pore MCP's.

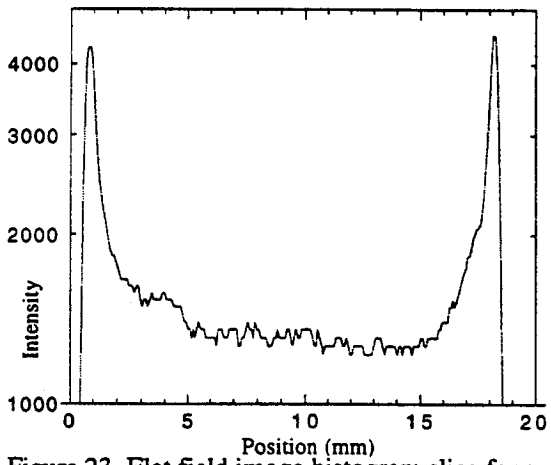

Figure 23. Flat field image histogram slice for a 4 MCP stack of Philips 6μm pore MCP's.

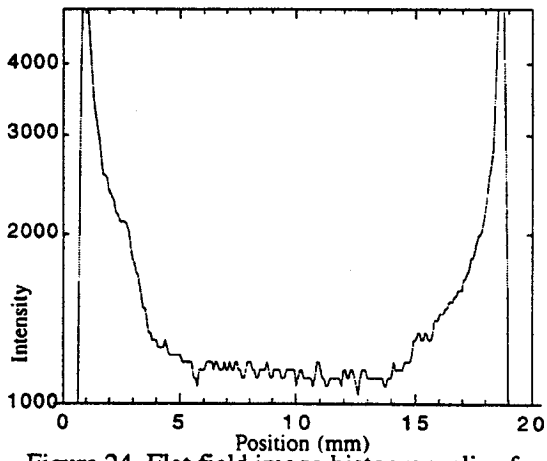

Figure 24. Flat field image histogram slice for a 4 MCP stack of Philips 7μm pore MCP's.

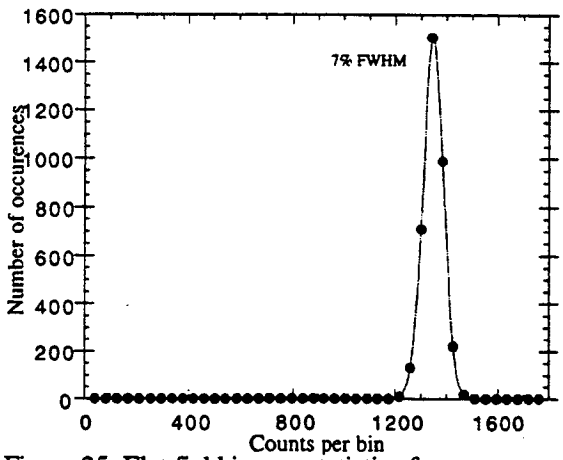

Figure 25. Flat field image statistics for a 4 MCP stack of Philips 6μm pore MCP's.

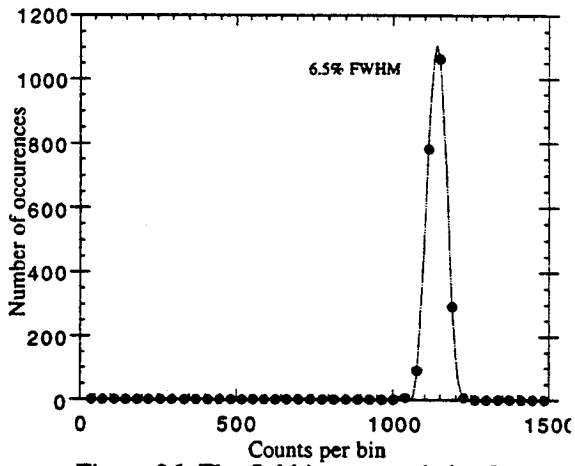

Figure 26. Flat field image statistics for a 4 MCP stack of Philips 7μm pore MCP's.

the small pore MCP's is 60% to 65% for all the MCP's, compared with ≈65% for normal 10μm and 12.5μm pore MCP's. Therefore there are no obvious changes in the open area ratio and this does not seem to be an issue. Over the past few years we have noticed on a number of occasions that the QDE of some batches of MCP's that the QDE was significantly below that expected. After a considerable amount of study we have established that the actual QDE of the photoemitting surfaces is probably not degraded. We surmise that problem is possibly due to inefficient detection of the emitted photoelectrons by the MCP (electron detection probability in Ref 10). We are currently attempting to resolve this problem with the manufacturers and will report on this at a future date.

3.5 Flat field characteristics

Deep flat field images (>1000 events/pixel) for the 6μm and 7μm MCP stacks were obtained under illumination with 2537Å light (Hg vapor lamp). The contrast enhanced flat field response of the 6μm and 7μm MCP stacks are shown in Figures 21 and 22 respectively. Flat field images were acquired at rates of ≈10,000 events/sec, and binned into a 128x128, 125μm bin format. The only visible flat field modulation effects are the edge intensity enhancements due to reflections of light by the detector clamps. Typically the dominating modulation seen in flat field images is that of the MCP multifibers. MCP modulation at the multifiber boundaries is usually of the order 10%-15%[11]. It is unusual that these MCP's do not show the MCP multifiber structure. Earlier results have linked the MCP multifiber modulation to physical distortions of the MCP pores at the boundaries of the multifibers[11].

Histograms of the intensity maps for the images in Figures 21 and 22 are shown in Figs. 23 and 24 respectively. The intensity variations in the central areas are small and have no scale length pattern correlations. The statistical variations of the flat field intensity in the central 5mm of the images are shown in Figures 25 and 26. The expected variations are 6.5% and 6.9% FWHM for the 6μm and 7μm flat fields respectively. The measured values are very close to those expected, which also confirms that there is little multifiber modulation.

4.0 ACKNOWLEDGMENTS

Many grateful thanks are extended to the many unmentioned people who contributed to this effort at U.C. Berkeley, this work was supported by NASA grants NAGW-2640 and NAGW-1290.

5.0 REFERENCES

1. Sahnow, D. C. Bowers, O.H.W. Siegmund, J. Stock, and M.A. Gummin, *Proc. SPIE*, 1945, 390-397, (1993)
2. O.H.W. Siegmund, M.A. Gummin, J. Stock, D. Marsh, R. Raffanti, and J. Hull, *Proc. SPIE*, 2006, 176-187 (1993).
3. Siegmund, O.H.W., Vallerga, J., and Wargelin, B., *IEEE Trans. Nucl. Sci.* , NS-35, 524 (1988).
4. Fraser, G.W., Pearson, J.F., and Lees, J.E., *Nucl. Instrum. & Meth.*, A254, 447 (1987).
5. Slater, D.C., and J.G. Timothy, *Proc. SPIE*, 1549, 68 (1991).
6. Siegmund. O.H.W., and J.Stock, *Proc. SPIE*, 1549, 81-89 (1991).
7. Fraser, G. W., Pain, M.T., Lees, J. E., Pearson, J. F., *Nucl. Instrum. & Meth. A*, preprint (1991).
8. Siegmund, O. H. W. M. A. Gummin, T. Sasseen, P. Jelinsky, G. A. Gaines, J. Hull, . M. Stock, M. Edgar, B. Welsh, S. Jelinsky, and J. Vallerga, *Proc. SPIE*, **2518**, 344-355, (1995)
9. Siegmund, O.H.W., K. Coburn, and R.F. Malina, *IEEE Trans. Nucl. Sci.* NS-32, 443-447 (1985).
10. Siegmund, O.H.W. E. Everman, J. Vallerga, J. Sokolowski, and M. Lampton, *Applied Optics*, 26(17), 3607 - 3614 (1987).
11. Vallerga, J.V., Siegmund, O.H.W., Vedder, P.W., Gibson, J., *Nucl. Instrum. & Meth.* A310, 317-322 (1991).